

Block-Diagonal Orthogonal Relation and Matrix Entity for Knowledge Graph Embedding

Yihua Zhu^{1,2} Hidetoshi Shimodaira^{1,2}

¹Kyoto University ²RIKEN

zhu.yihua.22h@st.kyoto-u.ac.jp, shimo@i.kyoto-u.ac.jp

Abstract

The primary aim of Knowledge Graph embeddings (KGE) is to learn low-dimensional representations of entities and relations for predicting missing facts. While rotation-based methods like RotatE (Sun et al., 2019) and QuatE (Zhang et al., 2019) perform well in KGE, they face two challenges: limited model flexibility requiring proportional increases in relation size with entity dimension, and difficulties in generalizing the model for higher-dimensional rotations. To address these issues, we introduce OrthogonalE, a novel KGE model employing matrices for entities and block-diagonal orthogonal matrices with Riemannian optimization for relations. This approach enhances the generality and flexibility of KGE models. The experimental results indicate that our new KGE model, OrthogonalE, is both general and flexible, significantly outperforming state-of-the-art KGE models while substantially reducing the number of relation parameters. Our code is available at [OrthogonalE](#)

1 Introduction

The fundamental elements of knowledge graphs (KGs) are factual triples, each represented as (h, r, t) , indicating a relationship r between head entity h and tail entity t . Notable examples include Freebase (Bollacker et al., 2008), Yago (Suchanek et al., 2007), and WordNet (Miller, 1995). KGs have practical applications in diverse fields such as question-answering (Hao et al., 2017), information retrieval (Xiong et al., 2017), recommender systems (Zhang et al., 2016), and natural language processing (Yang and Mitchell, 2019), garnering considerable interest in academic and commercial research.

Addressing the inherent incompleteness of KGs, link prediction has become a pivotal area of focus. Recent research (Bordes et al., 2013; Trouillon et al., 2016) has extensively leveraged Knowledge Graph Embedding (KGE) techniques, aiming to

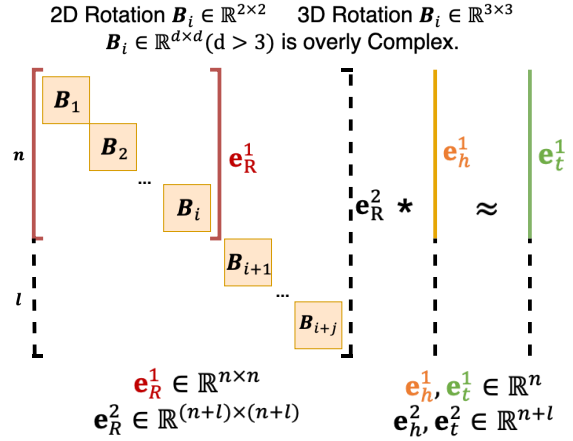


Figure 1: Fundamental operations and inherent challenges of rotation-based KGE models.

learn compact, low-dimensional representations of entities and relations. These approaches, marked by scalability and efficiency, have shown proficiency in modeling and deducing KG entities and relations from existing facts.

Recently, rotation-based KGE methods have achieved notable success in the field. For instance, RotatE (Sun et al., 2019) conceptualizes relations as 2D rotations, while QuatE (Zhang et al., 2019) employs 3D rotations. Essentially, as illustrated in Fig. 1, both operate by multiplying the relation matrix $e_R^1 \in \mathbb{R}^{n \times n}$ composed of numerous small rotation blocks $B_i \in \mathbb{R}^{d \times d}$ (RotatE: $\mathbb{R}^{2 \times 2}$, QuatE: $\mathbb{R}^{3 \times 3}$) with the head entity vector $e_h^1 \in \mathbb{R}^n$.

Nevertheless, these approaches encounter two primary issues as shown in Fig. 1. First, the model’s lack of flexibility necessitates increasing the overall relation matrix ($e_R^1 \in \mathbb{R}^{n \times n} \rightarrow e_R^2 \in \mathbb{R}^{(n+l) \times (n+l)}$) to meet entity dimension requirements ($e_h^1 \in \mathbb{R}^n \rightarrow e_h^2 \in \mathbb{R}^{n+l}$) for better represent entities, which often leads to redundancy and inefficiency in representing relations. Second, exploring high-dimensional rotational KGE models is challenging due to the significant computational de-

mands and complexity of rotations in higher dimensions ($\mathbf{B}_i : \mathbb{R}^{2 \times 2}, \mathbb{R}^{3 \times 3} \rightarrow \mathbb{R}^{d \times d}, d > 3$), such as 4D and 5D rotation. This restricts the development of more generalized and higher-dimensional rotation KGE approaches.

To overcome these issues, we propose a highly general and flexible KGE model named OrthogonalE as shown in Fig. 3. Firstly, by transforming entity vectors $\mathbf{e}_h \in \mathbb{R}^n$ into matrices $\mathbf{e}_H \in \mathbb{R}^{n \times m}$, we control the entity dimension through variable m , avoiding unnecessary expansion of the relation size. Secondly, leveraging the concept that rotation matrices are orthogonal, we replace rotation matrices \mathbf{B}_i with orthogonal matrices $\mathbf{X}_i \in \mathbb{R}^{d \times d}$ of adaptable dimensions d , facilitating the exploration of higher-dimensional block-diagonal orthogonal matrix models. Lastly, for effective optimization, we employ Riemannian optimization for the relation matrix $\mathbf{e}_R \in \mathbb{R}^{n \times n}$ and Stochastic Gradient Descent (SGD) for the entity matrix $\mathbf{e}_V \in \mathbb{R}^{n \times m}$.

We evaluate the new model on two KGE datasets including WN18RR (Dettmers et al., 2018), FB15K-237 (Toutanova and Chen, 2015). The experimental results demonstrate that our new KGE model, OrthogonalE, is both general and flexible, significantly outperforming state-of-the-art KGE models while substantially reducing the number of relation parameters.

2 Related Work

Knowledge Graph Embedding Translation-based approaches are prominent in KGE, notably TransE (Bordes et al., 2013), which interprets relations as vector translations. TransH (Wang et al., 2014), TransR (Lin et al., 2015), and TransD (Ji et al., 2015) represent extensions of the translation-based method, building upon the foundational approach of TransE. ComplEx (Trouillon et al., 2016) advances this by embedding entities and relations in a complex space and using the Hermitian product for modeling antisymmetric patterns, a technique that has proven highly effective in learning KG representations. Inspired by ComplEx, RotatE (Sun et al., 2019) then innovated by treating relations as rotations in a complex vector space, capable of capturing varied relation patterns like symmetry and inversion. Following this, QuatE (Zhang et al., 2019) employed quaternion operations (3D rotations) for even better expressiveness than RotatE.

However, considering the two major disadvantages of rotation-based methods mentioned in the

Introduction 1, there is a need to refine our model to make it more general and flexible.

Optimization on the orthogonal manifold In optimization on the orthogonal manifold, transitioning from X^t to X^{t+1} while remaining on the manifold necessitates a method known as retraction (Absil and Malick, 2012). Prior research has effectively adapted several standard Euclidean function minimization algorithms to Riemannian manifolds. Notable examples include gradient descent ((Absil et al., 2008); (Zhang and Sra, 2016)), second-order quasi-Newton methods ((Absil et al., 2007); (Qi et al., 2010)), and stochastic approaches (Bonnabel, 2013), crucial in deep neural network training.

Riemannian Optimization has concurrently advanced in deep learning domains, particularly in CNNs and RNNs. (Cho and Lee, 2017) innovatively substituted CNN’s Batch Normalization layers with Riemannian optimization on the Grassmann manifold for parameter normalization. Additionally, significant strides in stabilizing RNN training have been made by (Vorontsov et al., 2017), (Wisdom et al., 2016), (Lezcano-Casado and Martinez-Rubio, 2019), and (Helfrich et al., 2018), through the application of Riemannian optimization to unitary matrices.

As this paper primarily focuses on KGE, we do not delve deeply into Riemannian optimization. Instead, we utilize the retraction with exponential map method for iterative optimization, sourced from the Geoopt (Kochurov et al., 2020).

3 Problem Formulation and Background

We present the KGE problem and describe Optimization on the orthogonal manifold before our approach part.

3.1 Knowledge Graph Embedding

In a KG consisting of fact triples $(h, r, t) \in \mathcal{E} \subseteq \mathcal{V} \times \mathcal{R} \times \mathcal{V}$, with \mathcal{V} and \mathcal{R} denoting entity and relation sets, the objective of KGE is to map entities $v \in \mathcal{V}$ to $k_{\mathcal{V}}$ -dimensional embeddings \mathbf{e}_v , and relations $r \in \mathcal{R}$ to $k_{\mathcal{R}}$ -dimensional embeddings \mathbf{e}_r .

A scoring function $s : \mathcal{V} \times \mathcal{R} \times \mathcal{V} \rightarrow \mathbb{R}$ evaluates the difference between transformed and target entities, quantified as a Euclidean distance:

$$d^E(\mathbf{x}, \mathbf{y}) = \|\mathbf{x} - \mathbf{y}\|$$

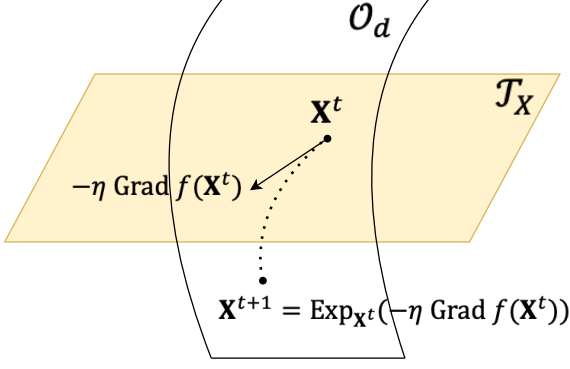


Figure 2: Abstract representation of Riemannian gradient descent iteration on orthogonal manifold

3.2 Optimization on the orthogonal manifold

In optimization on the orthogonal manifold, the core problem is formulated as:

$$\min_{X \in \mathcal{O}_d} f(X), \quad (1)$$

Here, f is a differentiable function mapping elements of $\mathbb{R}^{d \times d}$ to \mathbb{R} , and the *orthogonal manifold* \mathcal{O}_d is defined as $\mathcal{O}_d \triangleq \{X \in \mathbb{R}^{d \times d} \mid XX^\top = I_d\}$. Moreover, the tangent space at X , denoted by \mathcal{T}_X , is the set $\mathcal{T}_X = \{\xi \in \mathbb{R}^{d \times d} \mid \xi X^\top + X \xi^\top = 0\}$.

To address problem 1 more efficiently, recent studies suggest optimization on the orthogonal manifold with retractions as an effective approach (Ablin and Peyré, 2022). In this work, we primarily employ the retraction with exponential map method for iterative optimization, as illustrated in Figure 2. The key iteration formula for this method is:

$$X^{t+1} = \text{Exp}_{X^t}(-\eta \text{Grad} f(X^t)), \quad (2)$$

Where t indexes the iteration steps, $\text{Exp}_{X^t}(\xi)$ denotes the exponential map, and η represents the learning rate. $\text{Grad} f(\cdot)$ is the Riemannian gradient. Subsequent sections will delve into the computation of $\text{Exp}_{X^t}(\xi)$ and $\text{Grad} f(\cdot)$.

The exponential map allows movement in a specified direction on the manifold. Starting from X with initial velocity ξ , the exponential map for the orthogonal matrices manifold is represented by (Massart and Abrol, 2022):

$$\text{Exp}_X(\xi) = X \text{expm}(X^\top \xi), \forall \xi \in \mathcal{T}_X,$$

Where $\text{expm}(\cdot)$ denotes the matrix exponential.

On the orthogonal manifold, the Riemannian gradient $\text{Grad} f(\cdot)$ is calculated as (Absil et al., 2008):

$$\text{Grad} f(X) = P_{\mathcal{T}_X}(\nabla f(X)),$$

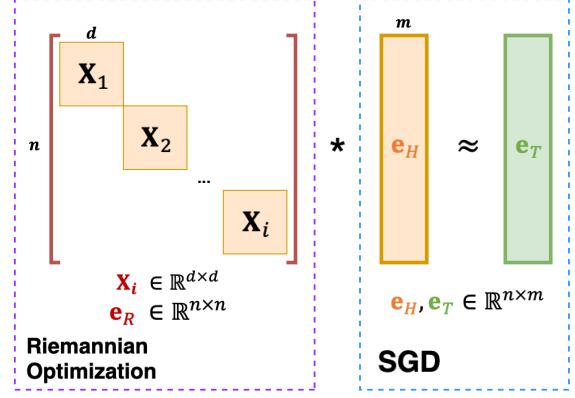


Figure 3: Diagram of the OrthogonalE approach.

Where $\nabla f(X)$ is Euclidean gradient of $f(X)$, and the calculation formula for $P_{\mathcal{T}_X}(\cdot)$ is:

$$P_{\mathcal{T}_X}(Y) = X \left(\frac{X^\top Y - Y^\top X}{2} \right), Y \in \mathbb{R}^{d \times d}$$

4 Approach

Our approach aims to acquire a flexible and general KGE model with employing matrices for entities and block-diagonal orthogonal matrices with Riemannian optimization for relations.

4.1 Orthogonal Matrices for Relations

RotatE (2D rotation) and QuatE (3D rotation) inherently employ fixed rotation matrices ($\mathbf{B}_i \in \mathbb{R}^{d \times d}, d \leq 3$), as depicted in Figure 1. However, the exploration of high-dimensional rotational KGE models ($\mathbf{B}_i \in \mathbb{R}^{d \times d}, d > 3$) is limited by substantial computational demands and the complexity of rotations in higher dimensions, which hinders the advancement of more generalized, high-dimensional rotational KGE models. To address this, we exploit the orthogonality of rotation matrices, substituting rotation matrices ($\mathbf{B}_i \in \mathbb{R}^{d \times d}$) with orthogonal matrices ($\mathbf{X}_i \in \mathbb{R}^{d \times d}$) of corresponding dimensions d . Consequently, our relation embedding ($\mathbf{e}_R \in \mathbb{R}^{n \times n}$) are composed of n/d block-diagonal orthogonal matrices \mathbf{X}_i as illustrated in Figure 3:

$$\mathbf{e}_R = \text{diag}(\mathbf{X}_1, \mathbf{X}_2, \dots, \mathbf{X}_{n/d}) \quad (3)$$

Where the number of relation parameters is $\frac{d(d-1)}{2} * \frac{n}{d} = \frac{(d-1)n}{2}$. And this aspect allows OrthogonalE to gain generality, adapting to datasets with diverse complexities by modifying the block-diagonal matrices' dimension d .

4.2 Matrices Representation for Entities

To enhance OrthogonalE’s flexibility, we aim to regulate entity dimension using variable m and transform entity vectors $\mathbf{e}_v \in \mathbb{R}^n$ into matrices $\mathbf{e}_V \in \mathbb{R}^{n \times m}$ as shown in Figure 3, thus preventing unnecessary expansion of the relation size. This part allows OrthogonalE to acquire flexibility, adapting to diverse datasets with varying relation and entity parameters, rather than indiscriminately increase both. And the number of entity parameters is $n * m$.

4.3 Scoring function and Loss

We utilize the Euclidean distance between the transformed head entity $\mathbf{e}_R \cdot \mathbf{e}_H$ and the tail entity \mathbf{e}_T as the scoring function:

$$s(h, r, t) = -d^E(\mathbf{e}_R \cdot \mathbf{e}_H, \mathbf{e}_T) + b_h + b_t \quad (4)$$

Here, $b_v (v \in \mathcal{V})$ denotes the entity bias, incorporated as a margin in the scoring function, following methodologies from (Tifrea et al., 2018; Balazevic et al., 2019). Furthermore, we opt for uniform selection of negative samples for a given triple (h, r, t) by altering the tail entity, rather than employing alternative negative sampling techniques. The loss function defined as follows:

$$L = \sum_{t'} \log(1 + \exp(y_{t'} \cdot s(h, r, t'))) \quad (5)$$

$$y_{t'} = \begin{cases} -1, & \text{if } t' = t \\ 1, & \text{otherwise} \end{cases}$$

4.4 Optimization

Traditional KGE models train and optimize relations and entities jointly. In contrast, our study aims for more effective optimization of the relation embeddings’ block-diagonal orthogonal matrices $\mathbf{X}_i \in \mathbb{R}^{d \times d}$ by separately optimizing relations and entities, utilizing Riemannian optimization for the relation matrix $\mathbf{e}_R \in \mathbb{R}^{n \times n}$ and SGD for the entity matrix $\mathbf{e}_V \in \mathbb{R}^{n \times m}$.

Initially, when optimizing relations, all entity parameters are fixed, rendering the entity embeddings analogous to the function $f(\cdot)$ in the problem 1. Notably, each orthogonal matrix \mathbf{X}_i within the relation embedding \mathbf{e}_R optimized by individual Riemannian optimization using RiemannianAdam (Kochurov et al., 2020), which is a Riemannian version (equation 2) of the popular Adam optimizer

Dataset	Entities	Relations	Train	Validation	Test
WN18RR	40,943	11	86,835	3,034	3,134
FB15k-237	14,541	237	272,115	17,535	20,466

Table 1: Details of the two datasets.

(Kingma and Ba, 2014). These are then concatenated in a block-diagonal way according to equation 3 to complete the process. After optimizing the relation parameters $\mathbf{e}_R \in \mathbb{R}^{n \times n}$, they are held constant while the entity parameters $\mathbf{e}_V \in \mathbb{R}^{n \times m}$ are optimized using Stochastic Gradient Descent (SGD), specifically employing the Adagrad optimizer (Duchi et al., 2011).

5 Experiment

We expect that our proposed OrthogonalE model, employing matrices for entities and block-diagonal orthogonal matrices with Riemannian optimization for relations, will outperform baseline models. Also, we anticipate OrthogonalE is a general and flexible KGE model that saves parameters while effectively balancing high-dimensional block-diagonal orthogonal matrices \mathbf{X}_i and entity matrices \mathbf{e}_V . Our goal is to validate these through empirical testing.

5.1 Experiment Setup

Dataset. We evaluate our proposed method on two KG datasets, including WN18RR (Dettmers et al., 2018), FB15K-237 (Toutanova and Chen, 2015). The details of these datasets are shown in Table 1.

Evaluation metrics. To predict the tail entity from a given head entity and relation, we rank the correct tail entity among all possible entities using two established ranking metrics. First is the Mean Reciprocal Rank (MRR), the average inverse ranking of correct entities, calculated as $\frac{1}{n} \sum_{i=1}^n \frac{1}{\text{Rank}_i}$. Second is Hits@K for $K \in \{1, 3, 10\}$, the frequency of correct entities ranking within the top K positions.

Baselines. We compare our new model with state-of-the-art (SOTA) methods, namely TransE (Bordes et al., 2013), DistMult (Yang et al., 2014), ComplEx (Trouillon et al., 2016), ConvE (Dettmers et al., 2018), RotatE (Sun et al., 2019), and QuatE (Zhang et al., 2019). In addition to these five and our OrthogonalE, we introduce comparative models utilizing the Gram-Schmidt process for generating orthogonal matrices and SGD for joint relation-

Model	WN18RR				FB15K-237			
	MRR	H@1	H@3	H@10	MRR	H@1	H@3	H@10
TransE \diamond	.226	-	-	.501	.294	-	-	.465
DistMult \diamond	.430	.390	.440	.490	.241	.155	.263	.419
ComplEx \diamond	.440	.410	.460	.510	.247	.158	.275	.428
ConvE \diamond	.430	.400	.440	.520	.325	.237	.356	.501
RotatE \diamond	.470	.422	.488	.565	.297	.480	.328	.205
QuatE \diamond	.481	.436	.500	.564	.311	.221	.342	.495
Gram-Schmidt(2×2)	.475	.434	.489	.556	.317	.226	.344	.502
Gram-Schmidt(3×3)	.487	<u>.445</u>	.500	.568	.322	.232	.350	.504
OrthogonalE(2×2)	<u>.490</u>	<u>.445</u>	<u>.503</u>	<u>.573</u>	<u>.330</u>	<u>.239</u>	.368	.516
OrthogonalE(3×3)	.493	.450	.508	.580	.331	.240	<u>.359</u>	<u>.513</u>

Table 2: Link prediction accuracy results of two datasets, **Bold** indicates the best score, and underline represents the second-best score. For a fair comparison, we standardized m at 1 for Gram-Schmidt and all OrthogonalE sizes. The entity dimension for WN18RR was set to approximately 500 (e.g. 501 for 3×3 blocks to ensure experimental feasibility), and around 1000 for FB15K-237. [\diamond]: Results are taken from (Zhang et al., 2019). The result of RotatE(Sun et al., 2019) and QuatE(Zhang et al., 2019) are reported without self-adversarial negative sampling and type-constraints respectively for fair comparison.

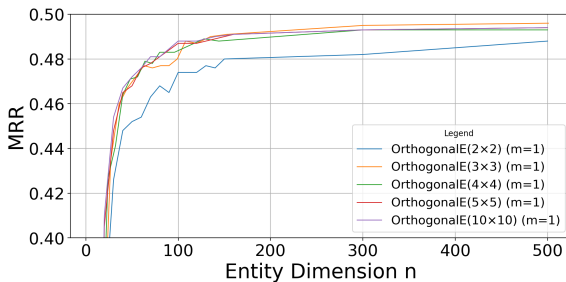


Figure 4: MRR accuracy comparison of OrthogonalE models with different small orthogonal matrices across varying entity dimensions ($n * 1$, we set $m = 1$) on WN18RR.

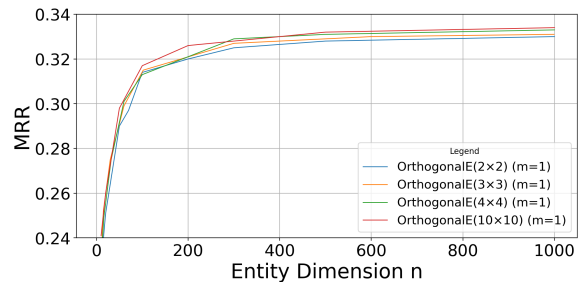


Figure 5: MRR accuracy comparison of OrthogonalE models with different small orthogonal matrices across varying entity dimensions ($n * 1$, we set $m = 1$) on FB15K-237.

entity training. OrthogonalE further differentiates by employing orthogonal matrices of varying sizes to discuss performance nuances.

Implementation The key hyperparameters in our implementation include the learning rate for RiemannianAdam (Kochurov et al., 2020) and Adagrad (Duchi et al., 2011), negative sample size, and batch size. To determine the optimal hyperparameters, we performed a grid search using the validation data.

5.2 Results

We first analyzed the overall accuracy for all baseline models and OrthogonalE, then separately examined the impacts of Block-diagonal Orthogonal matrices, Riemannian Optimization for relations,

and Entity matrices on the model from various experimental results. These results provided evidence supporting OrthogonalE’s generality and flexibility.

Overall Accuracy Table 2 presents link prediction accuracies for the WN18RR and FB15K-237 datasets. The OrthogonalE model surpasses all state-of-the-art models, highlighting its superior representational ability by employing matrices for entities and block-diagonal orthogonal matrices with Riemannian optimization for relations. Moreover, the OrthogonalE model with 2×2 and 3×3 configurations yields significantly better performance than corresponding sizes of the Gram-Schmidt method, and notably exceeds RotatE and QuatE, respectively, showcasing the enhanced efficacy of the KGE model.

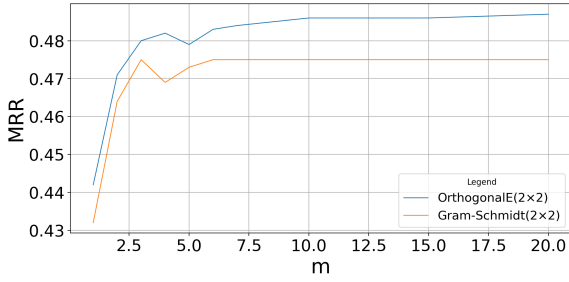


Figure 6: MRR accuracy comparison of OrthogonalE(2×2) and Gram-Schmidt(2×2) models across varying entity dimensions (m) with fixed relation matrix (40×40) on WN18RR.

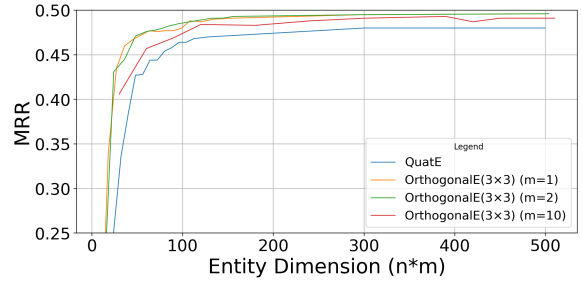


Figure 8: MRR accuracy comparison of QuatE and OrthogonalE(3×3) models across varying entity dimensions ($n * m$) on WN18RR.

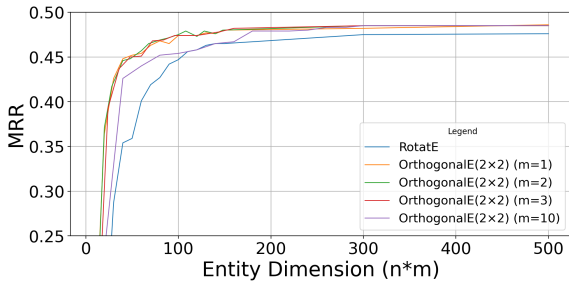


Figure 7: MRR accuracy comparison of RotatE and OrthogonalE(2×2) models across varying entity dimensions ($n * m$) on WN18RR.

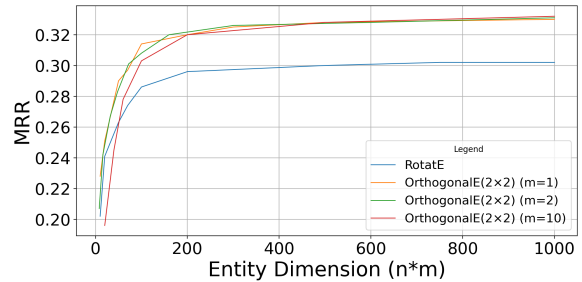


Figure 9: MRR accuracy comparison of RotatE and OrthogonalE(2×2) models across varying entity dimensions ($n * m$) on FB15K-237.

Block-diagonal Orthogonal matrices Figure 4 and 5 show MRR accuracy comparison of OrthogonalE models with different block-diagonal orthogonal matrices across varying entity dimensions ($n * 1$, we set $m = 1$) on WN18RR and FB15K-237, respectively.

An initial analysis of the datasets reveals that WN18RR contains 40,943 entities but only 11 relations, averaging 3,722 entities per relation. Conversely, FB15K-237 has 14,541 entities and 237 relations, averaging only 61 entities per relation. This suggests that WN18RR, in comparison to FB15K-237, requires a more complex and effective representation capability.

Our experimental findings align with the dataset analysis. For WN18RR, as shown in Figure 4, there is little difference in performance between 3×3 , 4×4 , 5×5 , and 10×10 blocks, but these configurations significantly outperform the 2×2 blocks. In contrast, for FB15K-237 depicted in Figure 5, the results across block-diagonal sizes, including 2×2 , 3×3 , 4×4 , and 10×10 are consistent. This suggests that 2×2 blocks suffice for representing FB15K-237’s relations, while WN18RR requires higher-dimensional, more complex blocks, such as

3×3 or 4×4 , for adequate representation. These results illustrate that the OrthogonalE model is general, which can adapt to datasets of various complexities by adjusting the dimension d of the block-diagonal matrices.

Riemannian Optimization for relations Figure 6 compares MRR accuracies of OrthogonalE (2×2) and Gram-Schmidt (2×2) across entity dimensions (m) with a constant relation matrix (40×40) on WN18RR, assessing the efficacy of orthogonal optimization beyond the Gram-Schmidt method for block-diagonal orthogonal matrices. The result demonstrates that OrthogonalE’s Riemannian optimization significantly exceeds Gram-Schmidt, underscoring its necessity.

Entity matrix Figures 7 and 8 compare MRR accuracies of RotatE with OrthogonalE (2×2) and QuatE with OrthogonalE (3×3) over different entity dimensions $n * m$ on WN18RR, then Figure 9 shows comparison of RotatE and OrthogonalE (2×2) in FB15-237. In OrthogonalE, we maintained a constant entity dimension ($n * m$) while varying m to assess the impact of entity shape. Figures 7 and 9 show that models with $m=1, 2$, or 3 (WN18RR) perform similarly and outperform

$m = 10$; notably, even when the number of relation parameters is just 1/10th of RotatE’s, the performance is significantly better at all dimensions. Figure 8 mirrors these findings, with $m=1$ and 2 outperform $m=10$, and $m=10$ again surpassing QuatE, which has 7.5 times more parameters. These results demonstrate OrthogonalE’s efficacy in saving relation parameters while outperforming RotatE and QuatE, highlighting our model’s flexibility in controlling entity dimension through variable m without unnecessarily increasing relation size.

Furthermore, Figure 6 result (with $m = 7$ yielding $MRR=0.483$) suggests that a relation matrix of 40×40 (20 parameters), compared to a dimension of 500 (250 parameters), can achieve comparably high performance, thus demonstrating that entity matrix method significantly reduces the need for excessive relation parameters to yield effective outcomes.

6 Conclusion

In this study, we propose the OrthogonalE model to acquire a flexible and general KGE model with employing matrices for entities and block-diagonal orthogonal matrices with Riemannian optimization for relations. The experimental results demonstrate that our new KGE model, OrthogonalE, is both general and flexible, significantly outperforming state-of-the-art KGE models while substantially reducing the number of relation parameters.

Acknowledgements

References

- Pierre Ablin and Gabriel Peyré. 2022. Fast and accurate optimization on the orthogonal manifold without retraction. In *International Conference on Artificial Intelligence and Statistics*, pages 5636–5657. PMLR.
- P-A Absil, Christopher G Baker, and Kyle A Gallivan. 2007. Trust-region methods on riemannian manifolds. *Foundations of Computational Mathematics*, 7:303–330.
- P-A Absil, Robert Mahony, and Rodolphe Sepulchre. 2008. *Optimization algorithms on matrix manifolds*. Princeton University Press.
- P-A Absil and Jérôme Malick. 2012. Projection-like retractions on matrix manifolds. *SIAM Journal on Optimization*, 22(1):135–158.
- Ivana Balazevic, Carl Allen, and Timothy Hospedales. 2019. Multi-relational poincaré graph embeddings. *Advances in Neural Information Processing Systems*, 32.
- Kurt Bollacker, Colin Evans, Praveen Paritosh, Tim Sturge, and Jamie Taylor. 2008. Freebase: a collaboratively created graph database for structuring human knowledge. In *Proceedings of the 2008 ACM SIGMOD international conference on Management of data*, pages 1247–1250.
- Silvère Bonnabel. 2013. Stochastic gradient descent on riemannian manifolds. *IEEE Transactions on Automatic Control*, 58(9):2217–2229.
- Antoine Bordes, Nicolas Usunier, Alberto Garcia-Duran, Jason Weston, and Oksana Yakhnenko. 2013. Translating embeddings for modeling multi-relational data. *Advances in neural information processing systems*, 26.
- Minhyung Cho and Jaehyung Lee. 2017. Riemannian approach to batch normalization. *Advances in Neural Information Processing Systems*, 30.
- Tim Dettmers, Pasquale Minervini, Pontus Stenetorp, and Sebastian Riedel. 2018. Convolutional 2d knowledge graph embeddings. *Proceedings of the AAAI conference on artificial intelligence*, 32(1).
- John Duchi, Elad Hazan, and Yoram Singer. 2011. Adaptive subgradient methods for online learning and stochastic optimization. *Journal of machine learning research*, 12(7).
- Yanchao Hao, Yuanzhe Zhang, Kang Liu, Shizhu He, Zhanyi Liu, Hua Wu, and Jun Zhao. 2017. An end-to-end model for question answering over knowledge base with cross-attention combining global knowledge. In *Proceedings of the 55th Annual Meeting of the Association for Computational Linguistics (Volume 1: Long Papers)*, pages 221–231.
- Kyle Helfrich, Devin Willmott, and Qiang Ye. 2018. Orthogonal recurrent neural networks with scaled cayley transform. In *International Conference on Machine Learning*, pages 1969–1978. PMLR.
- Guoliang Ji, Shizhu He, Liheng Xu, Kang Liu, and Jun Zhao. 2015. Knowledge graph embedding via dynamic mapping matrix. In *Proceedings of the 53rd annual meeting of the association for computational linguistics and the 7th international joint conference on natural language processing (volume 1: Long papers)*, pages 687–696.
- Diederik P Kingma and Jimmy Ba. 2014. Adam: A method for stochastic optimization. *arXiv preprint arXiv:1412.6980*.
- Max Kochurov, Rasul Karimov, and Serge Kozlukov. 2020. Geoopt: Riemannian optimization in pytorch. *arXiv preprint arXiv:2005.02819*.
- Mario Lezcano-Casado and David Martinez-Rubio. 2019. Cheap orthogonal constraints in neural networks: A simple parametrization of the orthogonal and unitary group. In *International Conference on Machine Learning*, pages 3794–3803. PMLR.

- Yankai Lin, Zhiyuan Liu, Maosong Sun, Yang Liu, and Xuan Zhu. 2015. Learning entity and relation embeddings for knowledge graph completion. *Proceedings of the AAAI conference on artificial intelligence*, 29(1).
- Estelle Massart and Vinayak Abrol. 2022. Coordinate descent on the orthogonal group for recurrent neural network training. In *Proceedings of the AAAI Conference on Artificial Intelligence*, volume 36, pages 7744–7751.
- George A Miller. 1995. Wordnet: a lexical database for english. *Communications of the ACM*, 38(11):39–41.
- Chunhong Qi, Kyle A Gallivan, and P-A Absil. 2010. Riemannian bfgs algorithm with applications. In *Recent Advances in Optimization and its Applications in Engineering: The 14th Belgian-French-German Conference on Optimization*, pages 183–192. Springer.
- Fabian M Suchanek, Gjergji Kasneci, and Gerhard Weikum. 2007. Yago: a core of semantic knowledge. In *Proceedings of the 16th international conference on World Wide Web*, pages 697–706.
- Zhiqing Sun, Zhi-Hong Deng, Jian-Yun Nie, and Jian Tang. 2019. Rotate: Knowledge graph embedding by relational rotation in complex space. *arXiv preprint arXiv:1902.10197*.
- Alexandru Tifrea, Gary Bécigneul, and Octavian-Eugen Ganea. 2018. Poincaré glove: Hyperbolic word embeddings. *arXiv preprint arXiv:1810.06546*.
- Kristina Toutanova and Danqi Chen. 2015. Observed versus latent features for knowledge base and text inference. In *Proceedings of the 3rd workshop on continuous vector space models and their compositionality*, pages 57–66.
- Théo Trouillon, Johannes Welbl, Sebastian Riedel, Éric Gaussier, and Guillaume Bouchard. 2016. Complex embeddings for simple link prediction. In *International conference on machine learning*, pages 2071–2080. PMLR.
- Eugene Vorontsov, Chiheb Trabelsi, Samuel Kadoury, and Chris Pal. 2017. On orthogonality and learning recurrent networks with long term dependencies. In *International Conference on Machine Learning*, pages 3570–3578. PMLR.
- Zhen Wang, Jianwen Zhang, Jianlin Feng, and Zheng Chen. 2014. Knowledge graph embedding by translating on hyperplanes. *Proceedings of the AAAI conference on artificial intelligence*, 28(1).
- Scott Wisdom, Thomas Powers, John Hershey, Jonathan Le Roux, and Les Atlas. 2016. Full-capacity unitary recurrent neural networks. *Advances in neural information processing systems*, 29.
- Chenyan Xiong, Russell Power, and Jamie Callan. 2017. Explicit semantic ranking for academic search via knowledge graph embedding. In *Proceedings of the 26th international conference on world wide web*, pages 1271–1279.
- Bishan Yang and Tom Mitchell. 2019. Leveraging knowledge bases in lstms for improving machine reading. *arXiv preprint arXiv:1902.09091*.
- Bishan Yang, Wen-tau Yih, Xiaodong He, Jianfeng Gao, and Li Deng. 2014. Embedding entities and relations for learning and inference in knowledge bases. *arXiv preprint arXiv:1412.6575*.
- Fuzheng Zhang, Nicholas Jing Yuan, Defu Lian, Xing Xie, and Wei-Ying Ma. 2016. Collaborative knowledge base embedding for recommender systems. In *Proceedings of the 22nd ACM SIGKDD international conference on knowledge discovery and data mining*, pages 353–362.
- Hongyi Zhang and Suvrit Sra. 2016. First-order methods for geodesically convex optimization. In *Conference on Learning Theory*, pages 1617–1638. PMLR.
- Shuai Zhang, Yi Tay, Lina Yao, and Qi Liu. 2019. Quaternion knowledge graph embeddings. *Advances in neural information processing systems*, 32.